Looking towards the use of a conceptual approach to predetermining high-return-period avalanche run-out distances

Maurice Meunier and Christophe Ancey

Cemagref
Research unit Torrential Erosion, Snow and Avalanche
Domaine universitaire BP 76
38402 Saint-Martin-d'Hères cedex, France

ABSTRACT. Investigating snow avalanches using a purely statistical approach raises several issues. First, even in the heavily populated areas of the Alps, there are few data on avalanche motion or extension. Second, most of the field data are related to the point of furthest reach in the avalanche path (run-out distance or altitude). As data of this kind are tightly dependent on the avalanche path profile, it is *a priori* not permissible to extrapolate the cumulative distribution function fitted to these data without severe restrictions or further assumptions. Using deterministic models is also problematic as these models are not really physically-based models. For instance, they do not include all the phenomena occurring in the avalanche movement, and the rheological behavior of the snow is not known. So, it is not easy to predetermine the extreme events extensions.
Here, in order to overcome this issue, we propose to use a conceptual approach. First, using an avalanche-dynamics numerical model, we fit the model parameters (friction coefficients and the volume of snow involved in the avalanches) to the field data. Then, using these parameters as random variables, we adjust appropriate statistical distributions. The last steps involve simulating a large number of (fictitious) avalanches using the Monte Carlo approach. In this way, the cumulative distribution function of the run-out distance can be computed over a much broader range than initially with the historic data. In this paper, we will develop the proposed method through a complete case study, using two different models for comparison.

I INTRODUCTION

This paper examines the possibility of using a conceptual approach to predetermining the run-out distance of rare avalanches (i.e., whose period of return is large, basically 100 yr or more). Conceptual approaches are common in hydrology, notably in the problems related to the predetermination of discharge in a given watershed from rainfall data. To our knowledge, approaches of this kind have never been fully attempted in the study of avalanche extensions although they can provide a more robust alternative to the statistical and deterministic (physical) approaches so far used for determining the run-out distance (point of furthest reach) of rare avalanches.

In the statistical approach, the basic ideas were expressed in the pioneering work of Lied and Bakkehøi (1980). The authors assumed a regional homogeneity in the avalanche behaviour for a given mountain range. This allowed them to pool the data from various paths in a common database. In this way, using regression techniques, they obtained the relationship between the run-out distances and various key variables of the path profile. This methodology has been applied to different mountain ranges over the world (see Bakkehøi and others, 1983; McClung and Lied, 1987; Fujisawa and others, 1993; Adjel, 1995) and extended to introduce the period of return as a parameter of the problem (McClung, 2000, 2001). In Alpine countries, where most of the time the avalanche paths of the same mountain range exhibit no similarity in their shape, the fundamental assumption of avalanche homogeneity is questionable (Adjel, 1995).

In the deterministic approach (for a review, see Harbitz, 1999; Ancey, 2001), the avalanche features are deduced from solving the equations of motion (mass and momentum equations). Deterministic models (sliding-block and depth-averaged models) introduce a friction law, reflecting the interaction between the avalanche and the path. In most models, the friction law includes two empirical frictional parameters, which have been fitted from field observations (Schaerer, 1975; Dent and Lang, 1980; Buser and Frutiger, 1980). The resulting values have been proposed as default values in engineering guidelines [Swiss guidelines on the so-called Voellmy-Salm-Gubler method (Salm and others, 1990) or the USGS handbook (Mears, 1992)]. Though it aims primarily at providing a physical picture of avalanche motion, the deterministic approach involves too many *ad hoc* assumptions to be considered as a true physical approach. Indeed, a number of basic physical processes (snow entrainment or release, turbulent suspension and transformation into an airborne, etc.) occurring in the avalanche course are either unknown or neglected in the avalanche-dynamics models. Furthermore, very little is known on the bulk rheological behaviour of snow and therefore, despite a number of attempts to find physical justifications for their expressions (e.g., see Salm, 1993), the friction laws used so far remain speculative and empirical. In this respect, it is not surprising that, in a recent benchmark of avalanche-dynamics models (see Barbolini and others, 2000), a significant mismatch was found in the frictional parameter values fitted from field data: this merely means that these parameters do not represent physical properties of snow (like a snow viscosity) but, on the contrary, they reflect the interrelated influences of snow, path profile, and model assumptions on the computations. Such a result is sufficiently

disturbing to question the use of avalanche-dynamics models to paths where no field data are available.

The diversity of approaches to studying avalanches are also encountered in hydrological sciences. Resulting from a wider practice and intense debates within a large and growing community, the ideas in hydrology about modelling are probably more precise: a clear distinction is made between statistical, physical, and conceptual models; see, for instance Betson and others (1989), Beven (1989), and the recent papers by O'Connel and Todini (1996), Van der Kwaak and Loague (2001), or Bates and Campbell (2001). Most of the time, selecting one of these approaches depends on the knowledge level of basic physical processes involved in the problem together with the number, quality, and type of available data. Both conceptual and physical approaches represent the catchment response to a rainfall as the result of basic processes (infiltration, storage, runoff, etc.) but in a very different way. In the physical models, the elementary processes are assumed to be known from scale-down experiments in the laboratory; the parameters introduced in the models represent physical properties that can be measured accurately and independently. On the contrary, in the conceptual models, the processes believed to be dominant in the hydrological response of a basin are idealized in the form of mathematical operators; the objective is to mimic the natural processes and not to explain them. In that case, the model parameters are purely empirical functions or values, which must be calibrated using the physical observable variables that are the object of the prediction.

A parallel can be helpfully drawn between the avalanche run-out problem and the rainfall-runoff transformation. In both cases, one has input and output variables, between which one tries to find a causal/functional relationship using a physical/conceptual model. A difference, which may be seen slight at first glance, exists however: for avalanches, the only available output information is the run-out distance, which presents the drawback to be path-dependent, while in flood hydrology, the selected output variable is the flow discharge, which is a truly physical variable, that is, independent of the river section at which it is measured. This difference in the output variable status has substantial implications in the model development since, in the latter case, it is mathematically licit to extrapolate the probability distribution to estimate flood discharges of long period of return whereas, in the former case, such an extrapolation cannot be done without further information. Another consequence is that, for floods, the model parameters remain constant for all the events whereas for avalanches, they should vary from one event to another one.

The objective pursued in this paper is to provide a proper way of extrapolating the probability distribution of run-out distances observed in a given avalanche path. Since the physical approach is disqualified for the reasons given above, we have developed a conceptual model. The basic idea is to determine the dependency between the probability distribution of input and output variables for a given path. Here this is done numerically using Monte Carlo simulations. As input variable, we will use the starting altitude and the snow volume involved in the avalanche. An avalanche will be idealized as a sliding block and we will use a Coulomb-like model (one parameter model) and a Voellmy-like model (two-parameter model) as the mathematical operators for mimicking the main features of avalanche motion. Compared to others approaches relying on Monte Carlo simulations (e.g., Keylock and others, 1999; Barbolini and others, 2001), the present method need not to use questionable assumptions (such regionalization of data) to specify the probability distributions of variables and parameters but, on the contrary, use the observed field data to deduce consistent probability distributions.

METHODOLOGY

If we have a time series of field data including the run-out distance x_{stop}, it is quite easy to deduce its empirical probability distribution. The point is that, most of the time, the time series covers a narrow period, typically a few decades. Therefore the largest period of return that can be evaluated in this way cannot exceed a few decades while avalanche zoning requires determining the run-out distance of long return-period avalanches, typically avalanches whose return period equals or exceeds 100 yr. Because the empirical probability distribution $P(x_{stop})$ is not smooth and x_{stop} depends on the path profile, it is not licit to directly extrapolate $P(x_{stop})$ to determine the quantiles associated with low probabilities. Here we develop a model that use available field data at best in order to properly extrapolate $P(x_{stop})$.

Figure 1 depicts the general framework that we shall use to reach our objective. The basic idea is to assume that there is a single functional relationship G between the run-out distance and other field data. This means that, for our method to apply, we need to have distinctive types of field data at our disposal. These other field data include the snowfalls preceding the avalanche, the starting point elevation, the released volume of snow, and so on. For the moment, we do not precise the type and number of these data but merely we refer to them

generically as the input variables Θ. The functional relationship G relates the run-out distance x_{stop} of a given (fictitious or real) event to the input variables Θ. Obviously there is not a one-to-one universal function linking x_{stop} to Θ: indeed, it is expected that G also depends on the topographical features of the path and on a set Π of internal or structural parameters, reflecting the diversity and variability of snow consistency and avalanche motion. We express this complex relationship in the following form: $x_{stop} = G(\Theta \,|\, \Pi; \text{path})$. Here, in order to take the path influence into account, we assume that the functional G is a mathematical operator resulting from the integration of a momentum equation along the path profile $y = f(s)$ (see below); in the following, we will use the short-cut notation: $x_{stop} = G(\Theta \,|\, \Pi)$. If the input variables Θ and/or the internal parameters Π are random, then the run-out distance is also a random variable. If we are able to adjust the internal parameters Π for the computed run-out distances to match the observed run-out distance, then it is possible, by using Monte Carlo simulations, to create a large number of fictitious events coherent with the observations. If the run-out distance sample is large enough, we can fit an empirical probability distribution and then accurately determine the quantile related to a low occurrence probability (e.g., as low as 0.01 or 0.005).

After outlining the general principles, we will explain how the method can be applied in practice. The method can be broken into four steps:

- The first step is devoted to selecting the input variables among all the available field data and fitting Π. Usually in the avalanche database, various types of information are available (snowfall, volume, etc.) but not all the information can be used. For instance, redundant or interrelated data must be left aside. In a similar way, data whose time series is not complete or not consistent with other time series cannot be kept as input variables of the model. Then, the different values of Π are adjusted for each documented events. Different strategies can be used to solve this inverse problem. In hydrology, a current practice is to use Bayesian inference to deduce $p(\Pi)$ from $p(\Theta)$ and $p(x_{stop})$, where $p(X)$ is the probability density function of the random variable X. Deterministic methods can be used equally for that purpose (e.g., see Ancey and others, 2003). Here we directly compute Π for each event and then we adjust a probability distribution to the resulting sample of values Π. A difficulty common to all these methods is that we have a single type of output variable whereas the

dimension of Π may be larger than unity. In the case where $\Pi = \{\pi_1 \cdots \pi_n\}$ with $n \geq 2$, then only one parameter π_i can be determined provided that others parameters π_j with $j \neq i$ are known; therefore, we have: $\pi_i = G^{-1}\left(x_{stop}, \Theta \,|\, \pi_j\right)$. In practice, using propagation operators involving a large number of internal parameters leads to substantial complications.

- In the second step, attention is paid to obtaining the probability density functions of the input variables $p(\Theta)$ and $p(\Pi)$ (if the latter has not been determined in the first step). Since the data are available, this merely means that we try to adjust usual probability distributions (Gumbel, Pearson, normal, etc.) from the selected field data.
- In the third step, Monte Carlo simulations are performed. For each fictitious event, random realizations of Π and Θ are generated from their respective probability density function.
- In the fourth step, the run-out distance is computed by applying the propagation operator to these random vectors and stocked. A very large sample of x_{stop} can be obtained in this way. We then deduce the empirical probability density function of x_{stop}. This function must approximately match the empirical distribution adjusted from the recorded distances but, since it results from a much larger sample, it extends over a wider range of probabilities. This allows us to accurately compute the quantile associated with a low non-exceedance probability. For instance, the run-out distance whose period of return is 500 yr (corresponding to a non-exceedance probability of 0.002) can be determined by generating 1000 events.

Propagation operator

In this paper, we will examine a propagation operator involving one or two internal parameters. Here an avalanche is idealized as a solid mass sliding along a curvilinear path and experiencing a frictional force F, possibly depending on θ and/or u. In a first approximation, we assume that the structure of this frictional force is identical whatever the path and the avalanche; only its parameters may vary from one event to another but they remain constant during all the course of an avalanche. The general expression of the momentum equation writes

$$\frac{du}{dt} = g\sin\theta - \frac{F(\theta,u)}{m} \qquad (1)$$

As initial conditions: we use $u(x_{start}) = 0$, where x_{start} is the starting-point abscissa. The momentum equation is integrated along the path profile $y = f(s)$, where y denotes the elevation and s the abscissa along a horizontal axis; x is a curvilinear abscissa taken from an arbitrary origin on the path profile: $x = \int_0^s (1 + f'^2(\sigma))^{-1/2} d\sigma$. After integrating the equation numerically, we look for the position of the stopping point, at which the avalanche velocity vanishes. We refer to this point as the run-out point or distance x_{stop}. In Eq. (1), two expressions of the frictional force have been tested:

- One-parameter expression (Coulomb-like model): the force F assumed to be slope dependent $F = \mu mg\cos\theta$, where $\Pi = \{\mu\}$ is the internal parameter, θ is the local slope, m is the avalanche mass.

- Two-parameter expression (Voellmy-like model), the force F is split into a slope-dependent term and a velocity-dependent term: $F = \mu mg\cos\theta + \kappa u^2$, where u is the avalanche velocity, and $\Pi = \{\mu, \kappa\}$ are the two internal parameters. The former contribution allows one to control the avalanche extent while the latter mainly influences the maximum velocity that the avalanche can reach. Moreover, it has often been recognized that the avalanche mass or volume often influences the force: the larger volume V, the lower its bulk friction. Thus, the parameter κ must be a function of the avalanche volume. For convenience, here we assume that this dependency can be written in the following form: $\kappa = g/(\xi H)$ where ξ is a friction coefficient and $H \propto \sqrt{V}$ is a typical length assumed to give an estimate of the mean flow depth of the avalanche. Using heuristic arguments presented in the appendix, we will use the following *ad hoc* relationship between H and V: $H = 2.5 + 5\times10^{-3} V^{1/2}$.

III APPLICATION

Selected avalanche path and data

For the study case, we have selected the Entremere avalanche path, which is situated on the left side of the Arve river in the Chamonix valley (France). This choice was motivated by two different considerations: first, the avalanche activity is considerable and regular; thus we have a fairly long time series of avalanche data on this path (approximately 100 years); second, the

upper part of the profile is sufficiently smooth and open for the avalanche dynamics to be rather simple and similar for each event. In the lower part of the profile, there is a sharp transition in the path slope since, at an elevation of approximately 1000 m, the path is very close to the horizontal (Fig. 2). This transition significantly affects avalanche motion since several avalanches stopped in the transition zone. In order to test the influence of the profile on the distribution of extreme run-out distances, we will also consider a modified path profile, for which the slope discontinuity was smoothed. The two profiles are depicted on Fig. 2.

The avalanche database includes 59 events since 1905. Not all of these events have been recorded; notably, the avalanches stopping in the upper part of the site were not taken into account. For the period 1905–1970, the observed data were the starting and stopping elevations and the deposit volume; in Table 1, 30 events are concerned but, for three of them, no information on the deposit volume is available. In Fig. 2, we have reported the different starting and stopping points of the 27 avalanche events for the period 1905–1970. Since 1971, the deposit volume has no longer been estimated. For the recent period (1970–2002), 29 events have been recorded and will not be used here.

Uncertainty on the run-out elevation varies with time. At the beginning of the 20th century, it probably exceeded ± 100 m while nowadays it is expected to be much lower (± 25 m). If we use distance rather than elevation to describe avalanche run-out, then uncertainty on the stopping point position is amplified for the path parts where the slope is low, typically here in the nearly horizontal part of the profile. We will not study the consequences of this uncertainty on our results, but we will study the confidence limits which are generated by the method itself.

Procedure with the Coulomb-like model and results

For the first step, we have chosen the input and output variables: the starting and run-out distances x_{start} and x_{stop}. By fitting the model, we have obtained the sample of friction parameters (see Table 1).

For the second step, we have first fitted the sample of x_{start} values. Since x_{start} is bounded, it is very convenient to use the beta distribution as the probability distribution. Figure 3 shows that the frequencies of the middle classes in the experimental values are higher than the fitted distribution. The experimental histogram is very irregular; for instance, for some classes, empirical frequency is zero. We have fitted a Gumbel distribution to the μ sample, as

shown in Fig. 4. The Gumbel distribution has been used in a first approximation; other possibilities will be explored later on.

In the third step, we have created large samples of x_{start} and μ values using a random number generation routine. As the experimental sample contains 27 events for 60 years, the simulated sample for 1000 years should contains 450 events. Figure 3 (respectively 4) shows the simulated values for x_{start} (resp. for μ). It is seen that these samples are very close to the theoretical distributions.

In the last step, we have used these two samples to generate 450 fictitious avalanches. The run-out distance of each event has been stored. As shown in Fig. 5, there is no much difference between the empirical probability distribution of the simulated run-out distances computed using the Coulomb-like model or the Voellmy-like model (see below). The simulated run-out distances match well the field data, except for the last four identical points (run-out distance at 2100 m). At this critical point, the path profile is nearly horizontal (river bed) and, as stated previously, uncertainty on the stopping point position is high. Thus, on the whole, we can reasonably think that the model correctly describes the past avalanche activity in the Entremere path.

The 500-yr run-out distance obtained is 2269 m. This result is unique since the model has only one parameter and we use a single distribution for x_{start} and μ. We will see later on what happens with different distributions.

Procedure with the Voellmy-like model and results

In the first step, we have computed the input and output variables together with the friction coefficients. The Voellmy-like model involves two input variables, the initial condition x_{start} value and the avalanche depth H. The model has two internal parameters (μ, ξ). Since we have only one output variable, the value of one of them must be kept constant for the inverse problem to be solved. In the following, we will use the following notation $(\xi \mid \mu)$ when it is considered that the parameter ξ is free while the other parameter μ is held constant for all the events occurring in the path. Figure 6 represents the values of the friction parameter ξ that have been deduced from the field data when the value of the other friction parameter μ is held constant for all the events. A very similar figure (not reported here) has been obtained when computing the μ values for a varying ξ parameter. In either case, the

figure exhibits outliers issued from the same events that we will ignore later on. It is also worth noticing that:

- the curve $\mu(\xi)$ is horizontal for low and large values of ξ. This gives a first argument for reducing the range of ξ values: μ being fairly constant for the lowest and largest ξ values, we can consider that ξ ranges from 500 to 10,000 without loss of generality. Others arguments below can be used to narrow this range further.
- the data scattering defines two event families (denoted first and second group on Fig. 6): for a given ξ, there is no continuum in the μ values but, on the contrary, we can observe two narrow ranges of possible values. This clear separation in the fitted μ values has been also observed on other paths when the Voellmy model is used in a deterministic way (Ancey and others, 2003) and no convincing explanation has been found.

In the second step, we have first verified that the input variables are independent and necessary. Most authors who used a sliding block model (or, in fact, any avalanche-dynamics model) did not consider the starting point position as a reliable dynamics parameter since the initial conditions would affect neither the steady-state solution nor the run-out distance. We have examined this point more precisely: for all the experimental events, we computed the run-out distances with several fixed values of ξ, the value of μ (fitted to the observed events), and a fixed x_{start} value. The mean difference between the recorded and simulated run-out distances has been found to vary as a function of the ξ value. For values of ξ as high as 1000 m/s², the mean difference is close to zero and, in this case, the starting point position need not to be considered as an input parameter. However, for $\xi > 1000$ m/s², this no longer holds. The mean difference increases substantially with ξ and can exceed 40 m for ξ>5000 m/s². In short, surprisingly enough and contrary to a common belief, it is necessary to include the input variable x_{start} in the computations since the run-out distance may depend on x_{start} for sufficiently large values of ξ. A beta distribution has been used to fit the x_{start} values. For the avalanche depth H, a Gumbel distribution fits the data well as shown in Fig. 7. Usually, hydrologists consider that the Gumbel distribution fits *annual maximum series* (AMS) samples better than *peak over threshold* (POT) samples. However, here, for the high values of our POT sample, the Gumbel distribution fits sufficiently (to the naked eye) for us to keep it.

Determining the statistical distributions on the $(\xi \mid \mu)$ and $(\mu \mid \xi)$ samples turns out to be intricate since it is not licit to use a one-peak distribution fitted to the data. The simplest approximation involves taking the sum of the two probability distributions fitted on each group. In this way, we shall obtain the one-variable conditional distribution of each parameter. In a previous investigation, we found that a probability distribution made up of two beta distributions fits the $(\mu \mid \xi)$ values well (Meunier and others, 2001). However, since in the following, we are also interested in determining the $(\xi \mid \mu)$ distribution, we find it simpler to fit a statistical model resulting from superposing two normal distributions on the $(\mu \mid \xi)$ and $(\ln \xi \mid \mu)$ values; here we use $(\ln \xi \mid \mu)$ rather than $(\xi \mid \mu)$ because the range of possible ξ values covers several orders of magnitudes. As shown in Fig. 6 for ξ, we have explored the entire range of possible values for the two parameters even though they may have no physical meaning for the practitioner. Figure 8 shows the cumulative distribution functions fitted to the $(\ln \xi \mid \mu)$ values. These figures call for several remarks:

- The existence of two event groups is fully conditioned by the μ value: for $\mu < 0.4$, the second group does not exist because, in this case, the computed run-out distances $x_{stop}(\xi \mid \mu)$ never match the field data.

- For extreme μ values (i.e., when $\mu \leq 0.225$ or $\mu \geq 0.5$), agreement between empirical and computed frequencies is poor: the empirical distribution is step-shaped while the fitted distribution tends to smooth abrupt variations in the ξ value.

- For these extreme μ values, the fitted double normal distributions are no longer parallel to the others, which implies that the curves intersect. This point is disturbing: if we keep them, inconsistent values will be generated when we apply the Monte Carlo method. Obviously this undesirable behaviour originates from the fact that the curve $\mu(\xi)$ flattens out when $\xi \ll 10$ m/s²: in that case, low variations in the μ value induce large variations in the ξ value.

This motivates us to reduce the μ range by removing values that provide non-parallel curves in Fig. 8. Since we use double normal distributions, this also means that we discard the μ values whenever both the mean $\overline{\xi}$ and the standard deviation σ_ξ of the $(\ln \xi \mid \mu)$

sample differ significantly from a set of selected values. Translated into a mathematical expression, this condition can be expressed as follows. If the condition:

$$F(\mu) = \left| \frac{d\overline{\xi}}{d\mu} + \frac{d\sigma_{\xi}}{d\mu} \right| \leq k$$

is not fulfilled, in which $k = 20$ for the first avalanche group and $k = 55$ for the second avalanche group, then the μ value must be left aside. Using this criterion, we found that μ must range from 0.23 to 0.46 for the first group while μ must fall within the range 0.43–0.55 for avalanches belonging to the second group (see Fig. 9). The same exercise was done by inverting the role of μ and ξ. The same analysis as previously gives the same conclusions and conduct to a similar criterion:

$$G(\xi) = \frac{d\overline{\mu}}{d\ln\xi} - 6\left| \frac{d\sigma_{\mu}}{d\ln\xi} \right| \geq k'$$

where $k' = 0.04$ for the first group and $k' = 0.025$ for the second. Note that here, because the derivatives of the mean and the standard deviation do not have the same order of magnitude, we multiply the derivative of the standard deviation by 6 in order to give the same weight to the two derivatives. Eventually, we find that the ξ range is 900–5000 m/s² for the first group of avalanches and 165–2800 m/s² for the second group. The resulting ranges of the friction parameters have been tabulated in Table 2.

The third step is much easier: for each input variable, it has consisted in randomly generating a sample of 450 values from its adjusted empirical probability distribution (see Fig. 2 for x_{start} and see Fig. 6 for H). In a similar way, 450 values of the internal parameters have been created from the different conditional distribution of $(\ln\xi \mid \mu)$ or $\mu \mid \xi$.

In the fourth step, the run-out distances have been computed and stored. Figure 10 reports the statistical distributions of the run-out distances obtained when using the $(\mu \mid \xi)$ samples. Let us examine what happens when we consider extreme events that could occur in the future or that could have occurred in the distant past. A key point is that the bundle of curves diverges for run-out distances in excess of the critical point (2100 m). Data scattering is pronounced (200 m for the 500-yr return period run-out distance) when the entire range of ξ

is considered. In contrast, when we focus our attention on the limited range of ξ determined previously, we found that the range of 500-yr run-out distance is narrow: approximately 50 m.

We have proceeded similarly with the $(\xi \mid \mu)$ sample. The results are reported in Fig. 11. The range for 500-year run-out distance is similar for the entire or limited ranges of μ (120 m against 90 m). However, the mean values for the practical range are somewhat different: larger for the $(\mu \mid \xi)$ simulations (2228 m) than for the $(\xi \mid \mu)$ simulations (2206 m). Yet, the difference is only 22 m (see Table 3).

To summarize, we conclude that:

(i) we may either use the $(\mu \mid \xi)$ or the $(\xi \mid \mu)$ sample.

(ii) the range of values for the fixed parameter is not completely free and the choice of the variation range is important: it leads to an uncertainty of 50 m for the $(\mu \mid \xi)$ sample against 90 m for the $(\xi \mid \mu)$ sample.

If we now compare these results with the 500-yr run-out distance obtained with the Coulomb-like model (2269 m), we see that the difference is approximately 50 m, the Coulomb-like model providing a larger distance.

COMPLEMENTARY ANALYSIS

Study of the modified profile with the Voellmy-like model

The previous developments have used the real profile whose final part is horizontal. In the Chamonix valley path profiles of this kind are frequent while in many other valleys in the French Alps, the slope variation is gentler. In order to test the conceptual approach in this case, we have defined a modified profile (see Fig. 2) and we have proceeded to the same calculations as before. The three first steps are the same as before; and the fourth step differs only by the path profile used in the propagation operator.

We only present the results for the $(\mu \mid \xi)$ possibility (see Fig. 12); the 500-yr run-out distances obtained using the alternative possibility are reported in Table 3. Comparing Figs 10 and 12 is interesting: the bundles of curves are very similar below the key point of the horizontal terminal part of the profile and differ frankly above this point (2100 m). The range

of results for the 500-yr return period run-out distances is very large for the entire range of ξ values (310 m) but very narrow for the limited range (40 m). It means that it is very important to use the ranges of practical values for the internal parameters and not the entire ranges.

Table 3 shows that, once again, the runt-out distance obtained using the $(\mu \mid \xi)$ values are larger than those obtained when the $(\xi \mid \mu)$ values have been used. The difference (73 m) is larger than for the flat profile (22 m). The Coulomb-like model gives a 500-yr return period run-out distance of 2382 m situated between the two evaluations with the Voellmy-like model (2347 and 2420 m). We can consider than in the conceptual approach, the use of each model is quite equivalent.

Study of the friction parameter distribution with the Coulomb-like model

In the conceptual approach, the variability of all the input variables and the friction parameter is reflected in the Monte Carlo simulations by their statistical distributions. Therefore, the choice of these distributions is of great importance, especially for the variables or the parameters that may reach large values (e.g., H or ξ in the Voellmy-like model) or come close to zero (e.g., μ in the two models). We shall not study this problem completely, but we will provide some indications in comparing the 500-yr return period obtained with the Coulomb-like model when we use the Gumbel and the normal distributions for the friction parameter μ. Figure 13 provides the non-exceeding probability of x_{stop} obtained using a normal distribution for μ (instead of a Gumbel distribution). If the two distributions provide similar results for the centre of the sample, they differ significantly for the extreme values, especially for the lower values of μ. The behaviour entails substantial modifications (see Table 3): the results are much larger with the normal distribution than with the Gumbel distribution (115 m for the real profile and 211 m for the modified profile). Theses differences are larger than the differences observed when comparing the Coulomb-like and Voellmy-like models.

The role of the friction parameter distribution turns out to be strategic in the conceptual approach. This problem needs further investigations on other profiles, for which a large number of documented data are available.

What should be the size of the simulated samples?

In the preceding calculations we have always kept the same samples of 450 random numbers which gave either the μ sample for the Coulomb-like model or the $(\mu \mid \xi)$ [or the $(\xi \mid \mu)$] samples for the Voellmy-like model. The results obtained so far depend only on the model and the profile. In Figs. 10–12, it can be seen that the curves vary quite irregularly, implying that the confidence limits are large. In order to estimate the computation accuracy (i.e. taking into account the random uncertainty), we are now looking for the size of the simulation samples needed to yield a confident estimation of the 500-yr run-out distance. To that end, we will exemplify the method proposed for assessing the confidence interval by considering a particular case: in the computation, we will use the Voellmy-like model, the modified path profile (since it was shown that it amplifies data scattering) and the conditional probability of $(\mu \mid \xi = 1024 \text{ m/s}^2)$. As stated earlier, when $\xi = 1024$ m/s², the influence of the starting position is sufficiently weak for us to ignore it in the simulations.

We proceeded as follows: we performed 10 Monte Carlo simulations. For each of them, 450 events were simulated (as previously but each time with different random numbers samples). Taken as a whole, these computations can be seen as either the simulation of the avalanche activity over a 10,000-yr interval or the reproducibility test of the avalanche activity over a 1000-yr interval. As example, the 500-yr return period of the height H computed with the 1000 years simulation is 7.5 m ± 1 m. The run-out distance distributions are reported in Fig. 14. Data scattering is substantial for individual samples and long periods of return. Similarly, the distribution related to the 10,000-yr interval is much smoother than individual distributions and provides an average trend around which the individual distributions vary. In this respect, the 10,000-yr distribution can be used to determine a quantile accurately while the individual distributions provide an idea of the possible variations around this value, that is, an estimate of the confidence limits. For instance, if we consider the 500-year quantile of the run-out distance, we infer from Fig. 14 that the mean value is 2406 m and the confidence interval is approximately 2280–2650 m. The outcome is not very different if we take a longer interval of time (20,000 yr): we obtain 2394 m instead of 2406; the absolute difference between the two predictions is only 12 m.

A practical rule emerges from this example: it is highly recommendable to compute the desired quantile from a very large sample of simulations. Typically, if one is interested in

determining the 500-yr return period avalanche, one should generate a sample corresponding to a continuous period of 10,000 years (or more).

Summary

Table 3 sums up all the results for the 500 years return period run-out distances. It leads to the following conclusions:

- the results obtained with the Coulomb-like model are larger with the normal distribution than with the Gumbel distribution. The difference ranges from 100 m with the real profile to 200 m with the modified profile.
- The results given by the Voellmy-like model are different according to the $(\mu \mid \xi)$ or the $(\xi \mid \mu)$ sample. The difference ranges from 20 to 70 m, less than the difference introduced by the choice of the friction parameter distribution.
- The results obtained with the two models are very similar except when using the normal distribution for the μ values with the Coulomb-like model.

CONCLUSION

In this paper we have developed a method to compute the run-out distances of long-return-period avalanches. Since this variable depends on both the path profile and the avalanche dynamics, it is not licit to compute high-return-period run-out distances merely by extrapolating an empirical distribution fitted on the observed values.

Here we have suggested using a conceptual avalanche-dynamics model and a four-step methodology. The first step involves choosing the input variables according to the available data and to calculate the parameters of the avalanche-dynamics model from the recorded historical events. The second step involves adjusting the statistical distributions of the input variables and of the model parameters. In the third step, Monte Carlo simulations are performed by making use of the previously determined statistical distributions. In this way, in the fourth step, we can generate a series of fictitious avalanches over a period of any duration. By taking a very long interval of time (typically 10,000 years), it is possible to obtain an accurate estimate of the run-out distance of a very rare avalanche (500-yr return period). This four-step methodology has been exemplified here using an avalanche path in the French Alps and two sliding-block models, the Coulomb-like and the Voellmy-like model.

We have shown that this methodology can be easily used with the Coulomb-like model, which needs only one frictional parameter. It is more complicated with the Voellmy-like model based on two frictional parameters. We have also demonstrated that the conceptual approach can be used with benefit in the avalanche field to compute a high return period event. An important result is that the statistical distribution of the friction parameter plays a central role in the final results. Its choice is crucial and further investigations are needed on this point. Furthermore, no significant difference is found in the extrapolated quantile x_{stop} when the Coulomb-like and Voellmy-like models are compared.

APPENDIX

The mean flow depth H can be estimated from the recorded avalanche volumes by using assumptions similar to the empirical arguments used for debris flows and which were roughly validated by Russian experiments (Meunier, 1991 p. 208):

(i) For natural flows, it exists a relationship between height and width, for which we may use a power law function. For water discharge, the exponent is zero for rectangular section, equal to 1 for triangular section, and less than 1 for convex sections. Here we suppose that the width of the avalanche flow W is a power function of the avalanche height: $W \propto H^{0.7}$. This argument is more doubtful for open slope avalanche, depending on the rheological behaviour of avalanche snow.

(ii) Similarly the length L of the avalanche flow is a power function of the avalanche height, but with a lower exponent: $L \propto H^{0.3}$. In doing so, we obtain a crude relationship between the avalanche volume and its height: $V \propto H^2$. This expression holds on average but not necessarily for any event.

(iii) We assume that the avalanche flow depth ranges from 2.5 m to 8 m.

(iv) The avalanche volume is assumed to be constant during the avalanche run and deposition (snow entrainment and compaction are ignored).

REFERENCES

Adjel, G. 1995. Méthodes statistiques pour la détermination de la distance d'arrêt maximale des avalanches. *La Houille Blanche,* **7**, 100–104. (in French).

Ancey, C. 2001. Snow avalanches. *In* N. J. Balmforth and A. Provenzalle, *eds*. *Geomorphological Fluid Mechanics: selected topics in geomorphological fluid mechanics*. Springer. Berlin.

Ancey C., M. Meunier, and D. Richard. The inverse problem in avalanche-dynamics model, *Wat. Res. Research*. To appear, 2003

BakkehØi S., U.Domaas, K.Lied. 1983. Calculation of snow avalanche run-out distance. *Ann. Glaciol.,* **4**, 24–30

Barbolini M., U. Gruber, C. J. Keylock, M. Naaim and F. Savi. 2000. Application of statistical and hydraulic-continuum dense snow avalanche models to five real European sites. *Cold Reg. Sci. Techn*., **31**, 133–149.

Barbolini M., F. Savi. 2001. *Estimate of uncertainties in avalanche hazard mapping. Ann. of Glaciology 32 2001, 299-305*

Bates B.C, E.P. Campbell, 2001. A Markov chain Monte Carlo scheme for parameter estimation and inference in conceptual rainfall-runoff modelling. *Water Resources Research*, vol.37, N°4, 937-947

Betson R.P., C.V. Ardis Jr, 1989. Implications for modelling surface-water hydrology. In *Hillslope Hydrology. Chapter 8*. Kirkby M.J. Editor. John Wiley & Sons. 295-323

Beven K., 1989. Changing ideas in hydrology – The case of physically-based models. *J. Hydrol*. 105. 157-172.

Buser, O. and H. Frutiger. 1980. Observed maximum run-out distance of snow avalanches and the determination of the friction coefficients ξ and μ *J. Glaciol.,* **26**, 121–130.

Dent, J. D. and T. E. Lang, 1980. Modelling of snow flow. *J. Glaciol.,* **26**, 131–140.

Fujizawa, K., R. Tsunaki and I. Kamishii. 1993. Estimating snow avalanche run-out distances from topographic data. *Ann. Glaciol.,* **18**, 239–244

Harbitz, K. 1999. A survey of computational models for snow avalanche motion. Fourth European Framework Programme (ENV4- CT96-0258) Avalanche Mapping, Model Validation and Warning Systems.

*Keylock, C.J., D. M. McClung and M. M. Magnusson. 1999. Avalanche risk mapping by simulation. J. Glaciol., **45**, 303–314.*

Lied, K. and S. BakkehØi. 1980. Empirical calculations of snow avalanche run-out distance based on topographic parameters. *J. Glaciol.,* **26**, 165–177.

Mears, A. I. 1992. Snow-avalanche hazard analysis for land-use planning and engineering. Bulletin 49. Colorado Geological Survey. Denver.

McClung, D. M. 2000. Extreme avalanche run-out in space and time. *Can. Geotech. J.,* **37**, 161–170.

McClung, D.M. 2001. Extreme avalanche run-out: a comparison of empirical models. *Can. Geotech. J.,* **38,** 1254–1265.

McClung, D.M. and K. Lied. 1987. Statistical and geometrical definition of snow avalanche run-out. *Cold Reg. Sci. Techn*., **13**, 107–119.

Meunier M.,1991. Elements d'hydraulique torrentielle. *Cemagref. Série Etudes*. *Montagne* n°1. 278 pages (in french).

Meunier, M., C. Ancey and M. Naaim 2001. Mise au point d'une méthode de prédétermination statistique des cotes d'arrêt d'avalanches. *La Houille Blanche*, **6**, 92–98. (in French).
O'Connel P.E., E. Todini, 1996. Modelling of rainfall, flow and mass transport in hydrological systems: an overview. *J. Hydrol.* 175, 3-16
Salm, B. 1993. Flow, flow transition and run-out distances of flowing avalanches. *Ann. Glaciol.,* **18**, 221–226.
Salm, B., A. Burkard and H. Gubler. 1990. Berechnung von Fliesslawinen: eine Anleitung für Pratiker mit Beispielen. Internal report 47. EISFL. Davos. (in German).
Schaerer, P.A. 1975. Friction coefficients and speed of flowing avalanches. *In Grindelwald conference proceeding* (April 1974). IAHS publication 114. 425–432.
VandKwaak J.E., K. Loague, 2001. Hydrologic response simulations for the R-5 catchment with a comprehensive physics-based model. *Water Resources Research*, Vol. 37, n°4, 999-1013

FIGURE CAPTIONS

Figure 1: Slope profile of the Entremere avalanche path.

Figure 2: Statistical distribution of the avalanche starting distances

Figure 3: Probability distribution of the μ values (Coulomb-like model)

Figure 4: Run-out distance statistical distributions obtained with the Coulomb-like model

Figure 5: Computed values of ξ values with fixed μ

Figure 6: Statistical distribution of the avalanche heights.

Figure 7: One variable conditional probability distribution of $(\xi \mid \mu)$ with fixed μ (Voellmy-like model).

Figure 8: Determination of the reduced range of μ for the Voellmy-like model (the arrows indicate the limit of validity of the criterion).

Figure 9: Run-out distance statistical distributions with the μ samples, different fixed values of ξ (in m/s²), and the real profile (Voellmy-like model)

Figure 10. Run-out distance statistical distributions with the ξ (in m/s²) samples, different fixed values of μ, and the real profile (Voellmy-like model)

Figure 11: Run-out distance statistical distributions with the μ samples, different fixed values of ξ (in m/s²), and the modified profile (Voellmy-like model).

Figure 12: Comparison of two distributions fitted on the μ values with the Coulomb-like model

Figure 13: Determination of the confidence limits of the run-out distances (Voellmy-like model)

TABLE CAPTIONS

Table 1: Avalanche data on the Entremere path and μ values for the Coulomb-like model

Table 2: Range of practical interest for the friction parameters (Voellmy-like model).

Table 3: Comparison of the 500-year run-out distances obtained with the two models and for the two profiles

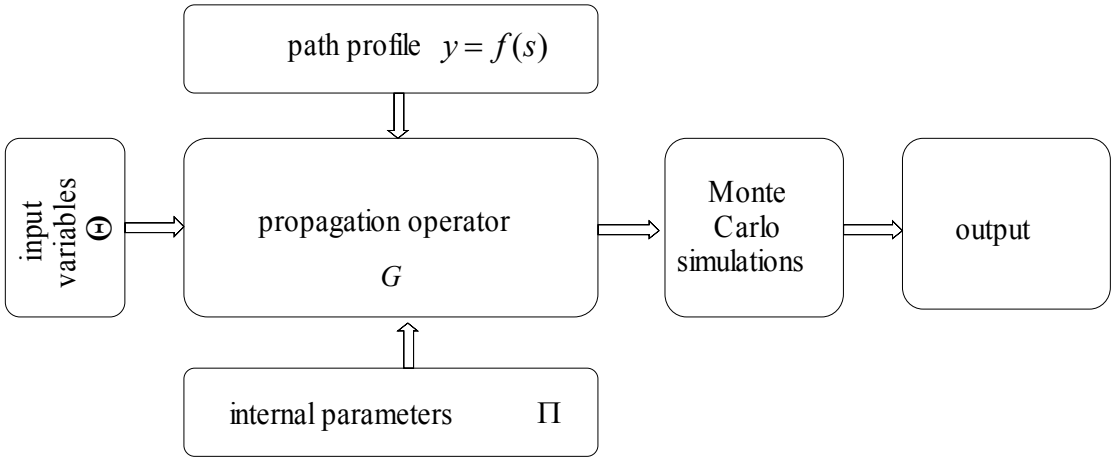

Figure 1: conceptual diagram of the approach.

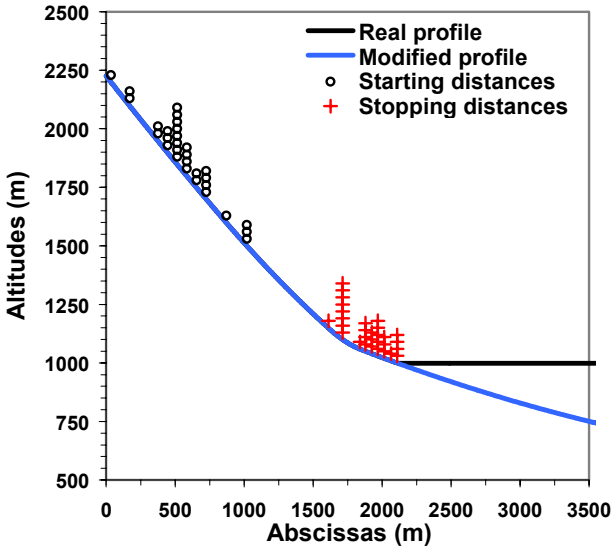

Figure 2: Slope profile of the Entremere avalanche path

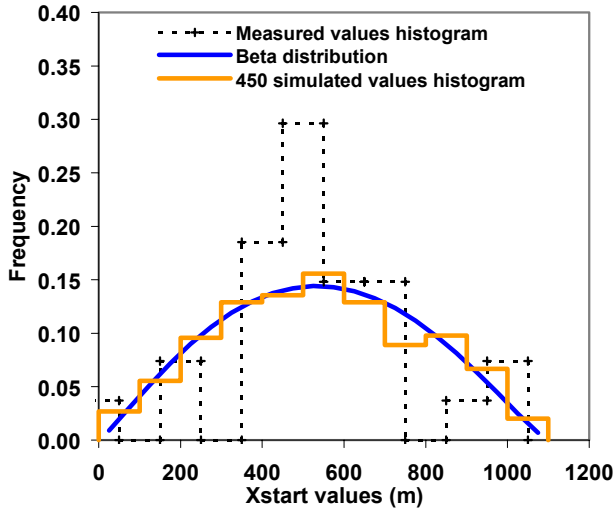

Figure 3: Statistical distribution of the avalanche starting distances

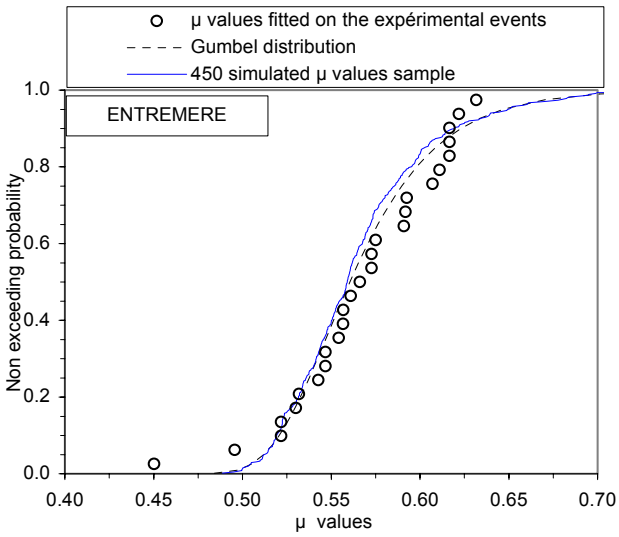

Figure 4: Probability distribution of the μ values (Coulomb-like model)

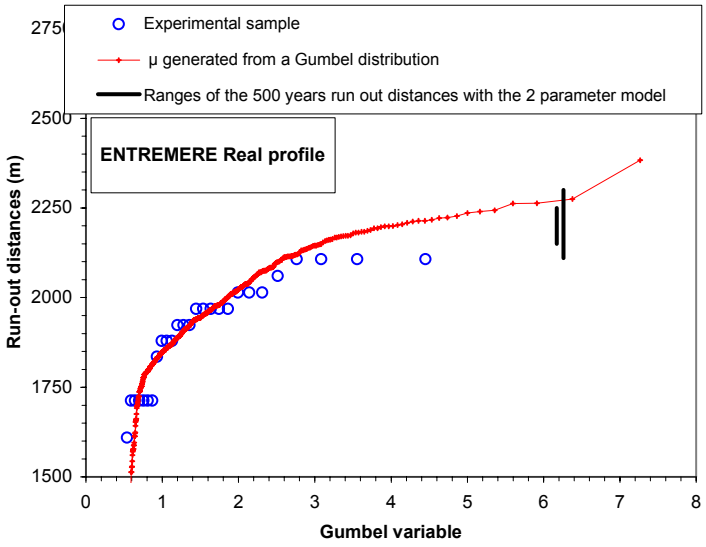

Figure 5: Run-out distance statistical distributions obtained with the Coulomb-like model

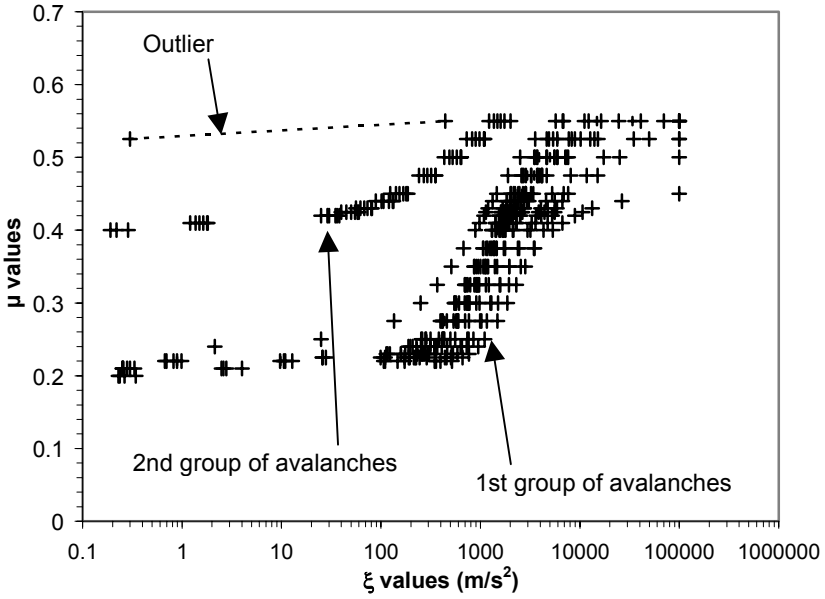

Figure 6: Computed ξ values with fixed μ

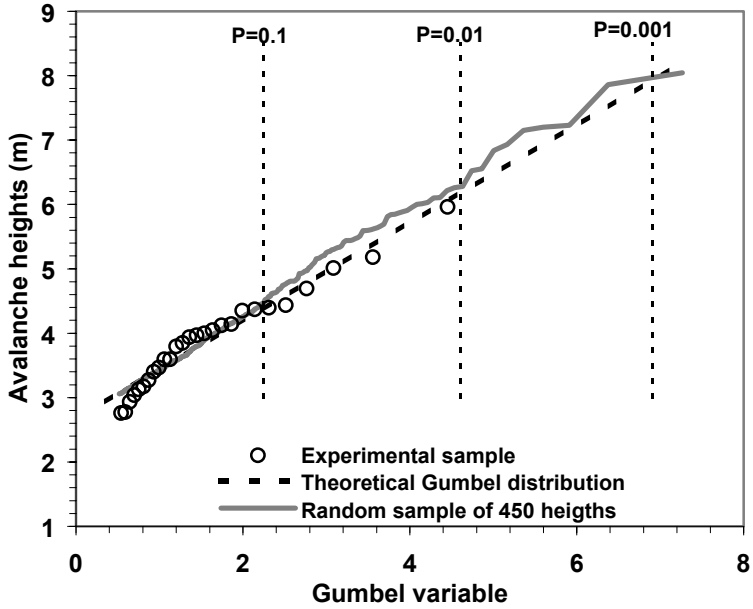

Figure 7: Statistical distribution of the avalanche heights

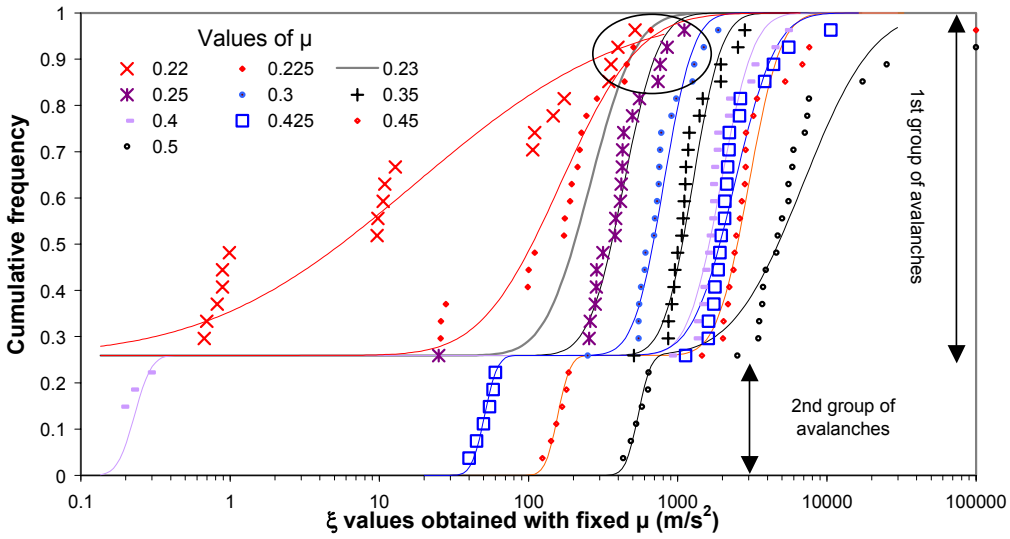

Figure 8: One variable conditional probability distribution of $(\xi \mid \mu)$ with fixed μ (Voellmy-like model)

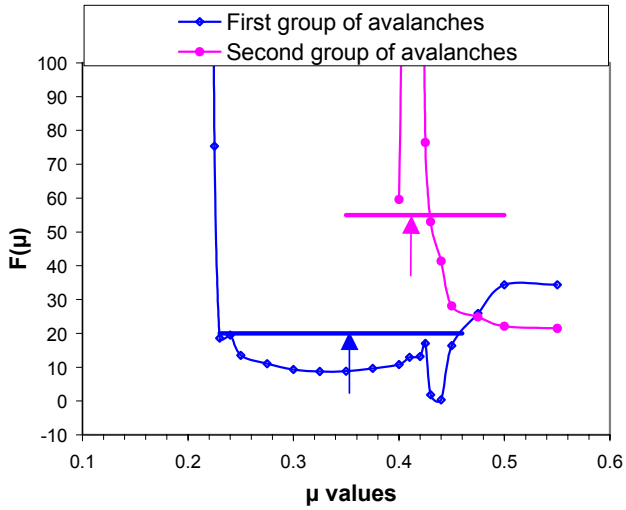

Figure 9: Determination of the reduced range of μ for the Voellmy-like model (the arrows indicate the limit of validity of the criterion)

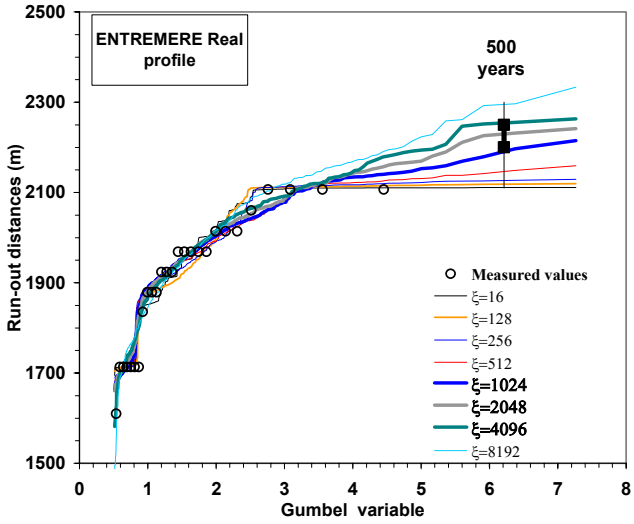

Figure 10: Run-out distance statistical distributions with the μ samples, different fixed values of ξ (in m/s²), and the real profile (Voellmy-like model).

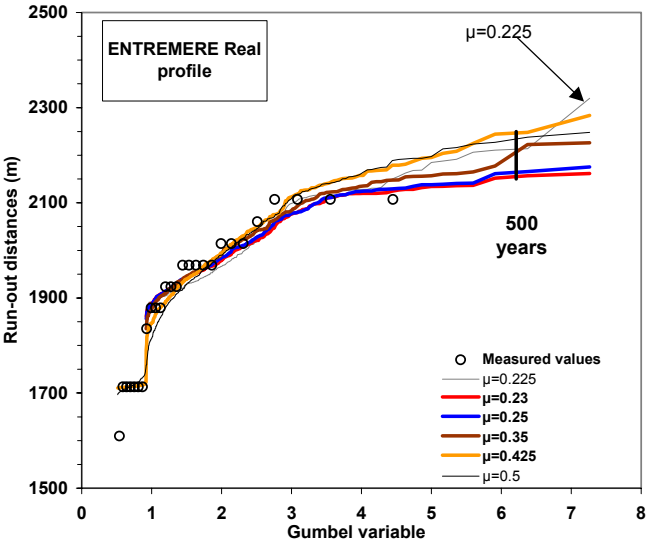

Figure 11: Run-out distance statistical distributions with the ξ (in m/s²) samples, different fixed values of μ, and the real profile (Voellmy-like model)

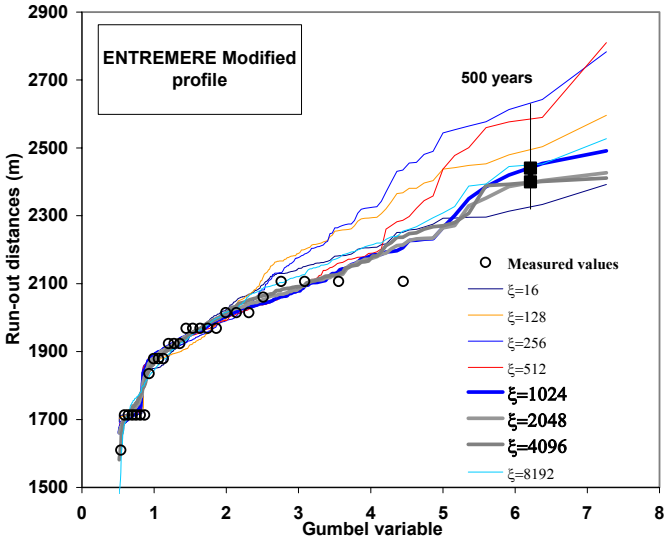

Figure 12: Run-out distance statistical distributions with the μ samples, different fixed values of ξ (in m/s²), and the modified profile (Voellmy-like model)

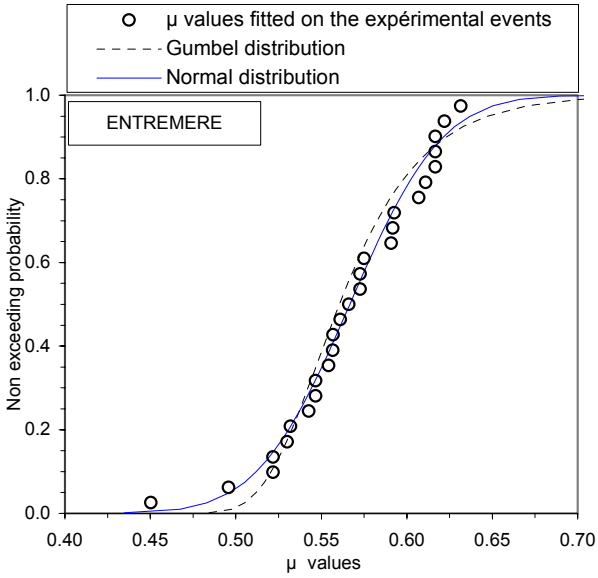

Figure 13: Comparison of two distributions fitted on the μ values with the Coulomb-like model

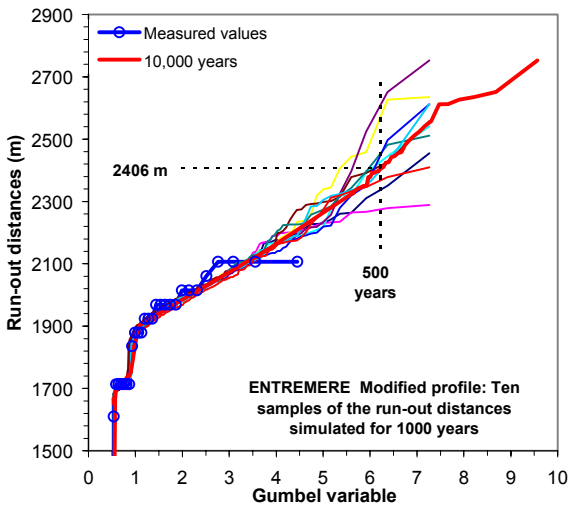

Figure 14: Determination of the confidence limits of the run-out distances (Voellmy-like model)

date	Zstart (m)	Zstop (m)	volume (m^3)	Coulomb-like model μ values
19/03/2005	2200	1050	3000	0.6167
14/01/2009	2100	1050	11520	0.6071
20/01/2010	1850	1010	478800	0.5319
18/11/2010	1800	1100	67200	0.6167
08/01/2012	1800	1030	32400	0.5468
23/01/2013	1850	1060	24000	0.5918
26-27/03/14	2100	1020	72960	0.5751
19/02/2016	1950	1020	252000	0.5567
28/03/2019	1900	1040	82500	0.5727
24-25/12/19	1850	1020	288000	0.5427
09/01/2022	1900	1040	136800	0.5727
02/03/2023	1850	1040	140000	0.5661
23/12/2023	1900	1030	150000	0.5610
27/12/2025	1850	1030	86400	0.5542
14/02/2028	1750	1100	192500	0.6111
31/01/2029	1950	1100	15750	0.6316
/04/35	1600	1100	18000	0.5909
12/01/1938	1850	1100	37500	0.6220
30/01/1938	1750	1100		
09/03/1939	1700	1050	7500	0.5568
02/01/1943	1700	1050		
08/12/1944	1700	1030	144000	0.5301
11-12/01/1947	1800	1100	105000	0.6167
09-10/02/50	1800	1030	96000	0.5468
20/01/1951	1850	1000	90000	0.5218
28/02/1952	1850	1000	2700	0.5218
24/02/1957	1500	1150	48000	0.5925
14/03/1958	1500	1000	48000	0.4503
29/03/1962	1500	1100		
03/02/1970	1700	1000	108000	0.4957

Table 1: Avalanche data on the Entremere path and μ values for the Coulomb-like model

	Practical range for μ in order to have ξ as a random variable	Practical field for ξ in order to have μ as a random variable
1st group of avalanches	**0.23–0.46**	**900–5000 m/s²**
2nd group of avalanches	**0.43–0.55**	**165–2800 m/s²**

Table 2: Range of practical interest for the friction parameters (Voellmy-like model)

	One parameter model			Two parameters model		
	1000 years simulation					
	Values of 500 years Xstop		Differences	Mean values of 500 years Xstop		Differences
	1) Normal law	2) Gumbel law	between 1 and 2	a) μ=0.23-0.46	b) ξ=900-5000 (m/s²)	between a) and b)
Real profile	2384	2269	115	2206	2228	-22
Modified profile	2595	2382	213	2347	2420	-73
	20000 years simulation					
	Values of 500 years Xstop		Differences	Mean values of 500 years Xstop		Differences
	1) Normal law	2) Gumbel law	between 1 and 2	a) μ=0.35	b) ξ=1024 (m/s²)	between a) and b)
Real profile	2360	2269	91	2205	2173	32
Modified profile	2547	2380	167	2320	2394	-74

Tableau 3: Comparison of the 500-year run-out distances obtained with the two models and for the two profiles